

## Nuclear magnetic resonance on oriented nuclei: Resonance shift with the external magnetic field

G. Seewald, E. Hagn, and E. Zech

Physik-Department, Technische Universität München, D-85748 Garching, Germany

(Received 24 October 1994)

We report measurements of nuclear magnetic resonance on oriented nuclei (NMR-ON) on  $^{99m}\text{Rh}$  ( $I^\pi = \frac{9}{2}^+$ ,  $T_{1/2} = 4.7$  h), and  $^{101m}\text{Rh}$  ( $I^\pi = \frac{9}{2}^+$ ,  $T_{1/2} = 4.3$  d) in Fe and Ni. The new measurements do not support the existence of a Knight shift of  $\sim -5\%$  for  $\text{RhFe}$  as postulated in the literature. The shift of the NMR-ON resonances with an external magnetic field is discussed critically, especially those effects which may simulate a Knight shift.

### I. INTRODUCTION

Since its discovery in 1966 by Matthias and Holliday,<sup>1</sup> the technique of nuclear magnetic resonance on oriented nuclei (NMR-ON) has been used for numerous precise determinations of the magnetic hyperfine splitting frequency  $\nu_M$  of radioactive nuclei in a ferromagnetic host lattice,

$$\nu_M = |g\mu_N B_{\text{HF}}/h|, \quad (1)$$

where  $g$  is the nuclear  $g$  factor and  $B_{\text{HF}}$  is the magnetic hyperfine field. In an external magnetic field  $B_{\text{ext}}$  the NMR-ON resonance frequency is given by

$$\nu = \nu_M + |g\mu_N B_{\text{ext}}(1+K)\text{sgn}(B_{\text{HF}})/h|. \quad (2)$$

Here  $\text{sgn}(B_{\text{HF}})$  is the sign of  $B_{\text{HF}}$  with respect to  $B_{\text{ext}}$ , and  $K$  is a parameter taking into account Knight shift and diamagnetic shielding. In experiment, the resonance frequency  $\nu$  is measured for different values of  $B_{\text{ext}}$ , and, assuming a linear dependence between  $\nu(B_{\text{ext}})$  and  $B_{\text{ext}}$ ,

$$\nu = [\nu(B_{\text{ext}}=0)] + [d\nu/dB_{\text{ext}}]B_{\text{ext}}, \quad (3)$$

$\nu(B_{\text{ext}}=0)$  and  $d\nu/dB_{\text{ext}}$  are determined with a *least-squares* fit. Under the assumption that  $\nu_M$  of Eq. (2) does not depend on  $B_{\text{ext}}$  the comparison of Eqs. (2) and (3) yields

$$|gB_{\text{HF}}| = \nu(B_{\text{ext}}=0)h/\mu_N \quad (4)$$

and

$$|g|(1+K) = |d\nu/dB_{\text{ext}}|h/\mu_N. \quad (5)$$

Combining Eqs. (4) and (5),

$$B_{\text{HF}}/(1+K) = \frac{\nu(B_{\text{ext}}=0)}{d\nu/dB_{\text{ext}}} \quad (6)$$

is obtained. Thus,  $B_{\text{HF}}/(1+K)$  can be determined experimentally without any further knowledge. This ratio is independent of  $g$ ; *redundant* information is obtained by measurements on different isotopes (with different  $g$ ).

The difference of  $K$  values for two different hosts, such as Fe and Ni, can be determined without any information on  $g$  factors and hyperfine fields from the resonance shifts

of the same isotope:

$$K^{(\text{Fe})} - K^{(\text{Ni})} \approx \frac{(1+K)^{(\text{Fe})}}{(1+K)^{(\text{Ni})}} - 1 = \frac{(d\nu/dB_{\text{ext}})^{(\text{Fe})}}{(d\nu/dB_{\text{ext}})^{(\text{Ni})}} - 1. \quad (7)$$

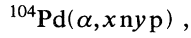
There have been several early reports about measurements on different impurity-host systems from which  $K$  values of a few percent were deduced which were attributed to a Knight shift.<sup>2,3</sup> Meanwhile, experimental resonance shift data in the literature and hence the deduced  $K$  values (which are often addressed as Knight shift) show a large scattering. Thus, there has been a continuous discussion whether the  $K$  values deduced from NMR-ON resonance shift measurements really represent the Knight shift or whether these  $K$  values are spurious results depending on the individual experiment. Recently, it was speculated that the resonance shift can be interpreted reliably only for measurements in very large external magnetic fields.<sup>4,5</sup>

We have viewed the literature for all resonance shifts which deviate from  $K=0$  by more than 1%. As the large deviations for  $^{191m}\text{IrNi}$  and  $^{192}\text{IrNi}$  (Ref. 3) have meanwhile been explained (Ref. 6; see also Sec. IV B), there remained only one case which seemed to be exceptional, namely Rh in Fe, for which several literature values grouped around  $K \sim -5\%$ .<sup>3,7-9</sup> Therefore we performed NMR-ON measurements on  $^{99m}\text{Rh}$  ( $I^\pi = 9/2^+$ ,  $T_{1/2} = 4.7$  h), and  $^{101m}\text{Rh}$  ( $I^\pi = 9/2^+$ ,  $T_{1/2} = 4.3$  d) in Fe and Ni in an external magnetic field up to 20 kG. To refute the speculation that the ("true") resonance shift can be obtained only from high-field resonances,<sup>4,5</sup> we have analyzed the resonance shift for different regions of the external magnetic field. The new measurements do not support the existence of a Knight shift of  $\sim -5\%$  for  $\text{RhFe}$ . In Sec. IV B we present an extensive discussion on those effects (fundamental and experimental) which may influence the shift of the NMR-ON resonances with an external magnetic field.

### II. EXPERIMENTAL DETAILS

The samples were prepared via recoil implantation at the cyclotron in Karlsruhe. A target stack consisting of

16~1 mg/cm<sup>2</sup> <sup>104</sup>Pd foils (enrichment 95.3%) each of which was followed by ~1 mg/cm<sup>2</sup> Fe (Ni) foil (purity 99.999%) was irradiated with 96 MeV  $\alpha$  particles ( $I=2$   $\mu$ A) for 8 h. Via the reaction



with  $x+y=7$  and 9, <sup>101m</sup>Rh and <sup>99m</sup>Rh are produced with a kinetic energy of ~3.5 MeV and are thus implanted homogeneously into the surface layers of the Fe (Ni) foils with a thickness of ~0.3  $\mu$ m. Via ( $\alpha, xnyp$ ) reactions in the Fe and Ni foils (contaminant) radioactive Co and Mn isotopes are produced. (Both, for Fe and Ni, the <sup>52</sup>Mn activity was sufficient for additional precise measurements of the <sup>52</sup>Mn NMR-ON resonance shift.) After the irradiations, the most active parts of the Fe (Ni) foils were soldered to the cold finger of a <sup>3</sup>He-<sup>4</sup>He-dilution refrigerator with top-loading facility, and cooled down to a temperature of ~10 mK. The  $\gamma$  rays were detected with four Ge detectors placed at 0°, 90°, 180°, and 270° with respect to the direction of the external magnetic field. The radio frequency was applied with a Marconi frequency synthesizer (model 2031).

The external magnetic field was supplied by a superconducting Helmholtz magnet working in persistent mode. Concerning the absolute (average) value of the external magnetic field at the nuclear sites there are two sources of error: (i) The nominal accuracy of the field calibration given by the manufacturer (Oxford Instruments) is  $\leq 1\%$ . For the verification of this calibration resonance shifts of isotopes have been measured for which the  $g$  factors are known precisely. (ii) The effective magnetic field at the sample site depends on geometrical effects, i.e., the (exact) positioning of different samples within the magnetic field. The respective uncertainty has been investigated by repeated measurements of the resonance shift on different samples. Taking into account the results of about 20 resonance shift measurements we estimate the upper limit for the total systematic error to be  $\lesssim 1\%$ . In order to give the right impression on the precision (and reproducibility) of the individual resonance shift measurements, this 1% systematic error is not included in the individual results. For the final results, however, the systematic error is included.

### III. RESULTS

#### A. <sup>101m</sup>RhFe

NMR-ON spectra were measured for  $B_{\text{ext}}=1, 3, 6, 8,$  and 11 kG. For  $B_{\text{ext}}=15$  and 20 kG, the rf power necessary for a considerable resonance destruction was so high that the temperature variation of the nonresonant heating varied considerably in the resonance region. This has the consequence that, because of the frequency dependence of the  $\gamma$  anisotropy, the *observed* resonance center is shifted in frequency. Therefore the 15 and 20 kG NMR-ON spectra were not included for the further analysis.

NMR-ON spectra measured for  $B_{\text{ext}}=1, 6,$  and 11 kG are shown in Fig. 1. The spectra indicate that <sup>101m</sup>Rh is substituted onto (at least) two different lattice sites. Therefore the spectra were interpreted with two Gauss-

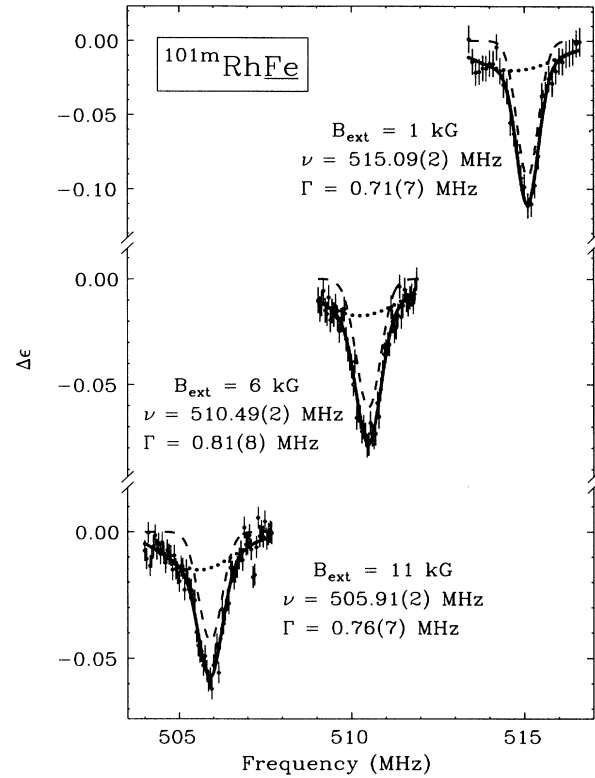


FIG. 1. NMR-ON resonances of the 307 keV transition of <sup>101m</sup>RhFe.

ian lines with different resonance centers and linewidths. The resonance with the small linewidths results from Rh nuclei on substitutional lattice sites with an undisturbed surrounding. The resonance with the larger linewidth must in our opinion be attributed to Rh nuclei on substitutional sites with a “moderately disturbed” surrounding, i.e., a defect in the (far) neighborhood.

The resonance centers and linewidths for the “narrow” resonance are listed in columns 2 and 3 of Table I. Interpreting the resonance centers according to Eq. (4) we get, taking the data for 1, 3, 6, 8, and 11 kG,

$$\nu(B_{\text{ext}}=0)=516.010(15) \text{ MHz},$$

$$d\nu/dB_{\text{ext}}=-0.9197(23) \text{ MHz/kG}.$$

TABLE I. NMR-ON results for <sup>101m</sup>RhFe (307 keV  $\gamma$  line) and <sup>52</sup>MnFe (average values for the 744, 935, and 1434 keV  $\gamma$  lines). The systematic error for the magnetic field (see text) is not included.

$B_{\text{ext}}$ (kG)	<sup>101m</sup> RhFe		<sup>52</sup> MnFe	
	$\nu_c$ (MHz)	$\Gamma$ (MHz)	$\nu_c$ (MHz)	$\Gamma$ (MHz)
1	515.093(20)	0.71(7)	88.357(6)	0.40(2)
3	513.254(14)	0.83(5)		
6	510.491(16)	0.81(8)	86.433(7)	0.46(2)
8	508.626(21)	0.87(7)		
11	505.906(18)	0.76(7)	84.494(11)	0.48(3)
20			80.983(14)	0.56(4)

Taking into account only the data for 3, 6, 8, and 11 kG, we obtain

$$\begin{aligned}\nu(B_{\text{ext}}=0) &= 516.008(20) \text{ MHz}, \\ d\nu/dB_{\text{ext}} &= -0.9195(28) \text{ MHz/kG},\end{aligned}$$

i.e., not different from the results from the full data set. For the linewidth, taking the full data set, we get

$$\begin{aligned}\Gamma(B_{\text{ext}}=0) &= 0.78(6) \text{ MHz}, \\ d\Gamma/dB_{\text{ext}} &= 0.003(9) \text{ MHz/kG}.\end{aligned}$$

This demonstrates that, as expected, the linewidth does not vary with the external magnetic field. The average linewidth is

$$\Gamma(^{101m}\text{RhFe}) = 0.80(3) \text{ MHz}.$$

The ratio of the linewidth to the zero-field splitting is

$$\Gamma/\nu_M(^{101m}\text{RhFe}) = 1.55(6) \times 10^{-3}.$$

### B. $^{52}\text{MnFe}$

The NMR-ON experiments on  $^{52}\text{MnFe}$  were performed after the  $^{101m}\text{RhFe}$  measurements without disassembling the cryostat. Here, it was easily possible to perform NMR-ON measurements up to  $B_{\text{ext}}=20$  kG. Spectra are shown in Fig. 2. These spectra could be well interpreted with one Gaussian line, i.e., the  $^{52}\text{Mn}$  nuclei

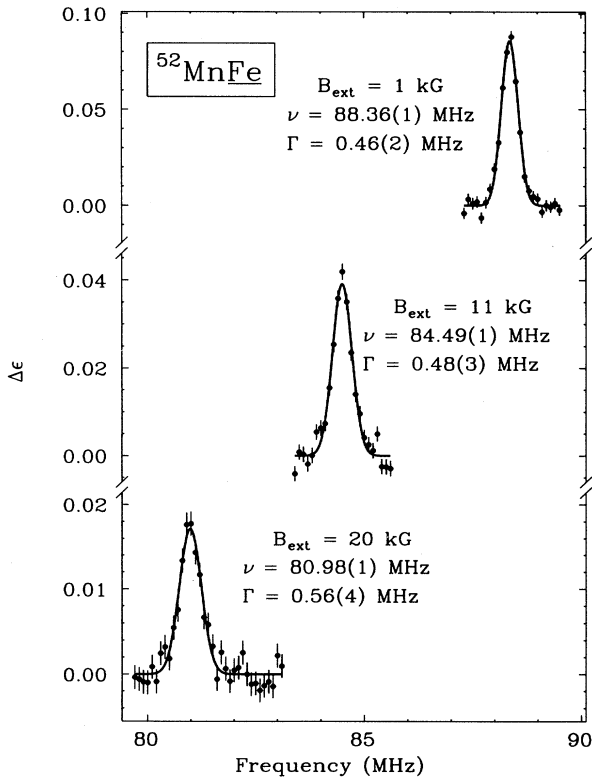


FIG. 2. NMR-ON resonances of  $^{52}\text{MnFe}$  (sum of 744, 935, and 1434 keV transitions).

are substituted onto one (unique) site, which must be a substitutional site with an undisturbed surrounding. The results are listed in columns 4 and 5 of Table I. Taking the data for 1, 6, 11, and 20 kG we get

$$\begin{aligned}\nu(B_{\text{ext}}=0) &= 88.750(5) \text{ MHz}, \\ d\nu/dB_{\text{ext}} &= -0.3874(8) \text{ MHz/kG}.\end{aligned}$$

Taking the data for  $B_{\text{ext}}=6, 11,$  and  $20$  kG, the results are

$$\begin{aligned}\nu(B_{\text{ext}}=0) &= 88.770(11) \text{ MHz}, \\ d\nu/dB_{\text{ext}} &= -0.3892(11) \text{ MHz/kG}.\end{aligned}$$

The resonance shift of the  $B_{\text{ext}} \geq 6$  kG data set is slightly higher than the shift of the full data set; the difference is  $5(4) \times 10^{-3}$ . The results for the  $^{52}\text{MnFe}$  linewidth are

$$\begin{aligned}\Gamma(B_{\text{ext}}=0) &= 0.40(2) \text{ MHz}, \\ d\Gamma/dB_{\text{ext}} &= 0.008(3) \text{ MHz/kG}.\end{aligned}$$

The linewidth shows a (very weak) increase with  $B_{\text{ext}}$ , which, however, should not be overinterpreted. Assuming that  $\Gamma$  is independent of  $B_{\text{ext}}$ , we get

$$\Gamma(^{52}\text{MnFe}) = 0.45(3) \text{ MHz}.$$

The ratio of the linewidth to the zero-field splitting is

$$\Gamma/\nu_M(^{52}\text{MnFe}) = 5.1(3) \times 10^{-3},$$

i.e., a factor of 3.3(2) larger than the corresponding ratio for  $^{101m}\text{Rh}$ , although both isotopes are in the same host matrix.

### C. $^{99m}\text{RhNi}$

Despite the short half-life of  $^{99m}\text{Rh}$  ( $T_{1/2}=4.7$  h), the NMR-ON resonances could be measured well for the Ni sample up to  $B_{\text{ext}}=15$  kG. The results are listed in columns 2 and 3 of Table II. For the zero-field splitting and the resonance shift we get, taking the full data set ( $B_{\text{ext}}=1, 3, 6, 9,$  and  $15$  kG)

$$\begin{aligned}\nu(B_{\text{ext}}=0) &= 215.965(2) \text{ MHz}, \\ d\nu/dB_{\text{ext}} &= -0.9480(32) \text{ MHz/kG}.\end{aligned}$$

Taking only the data for  $B_{\text{ext}}=3, 6, 9,$  and  $15$  kG, the results are

$$\begin{aligned}\nu(B_{\text{ext}}=0) &= 215.984(29) \text{ MHz}, \\ d\nu/dB_{\text{ext}} &= -0.9502(4) \text{ MHz/kG},\end{aligned}$$

i.e., the resonance shift is in good agreement with the shift of the full data set; the difference is  $2(5) \times 10^{-3}$ . Taking only the data for  $B_{\text{ext}}=6, 9,$  and  $15$  kG, the results are

$$\begin{aligned}\nu(B_{\text{ext}}=0) &= 216.034(51) \text{ MHz}, \\ d\nu/dB_{\text{ext}} &= -0.9551(57) \text{ MHz/kG}.\end{aligned}$$

The resonance shift agrees again with the shift of the full data set; the difference is  $7(7) \times 10^{-3}$ . The results for the

$^{99m}\text{RhNi}$  linewidth are

$$\Gamma(B_{\text{ext}}=0)=0.54(8) \text{ MHz} ,$$

$$d\Gamma/dB_{\text{ext}}=0.005(12) \text{ MHz/kG} .$$

The linewidth shows no increase with  $B_{\text{ext}}$ . The average linewidth is

$$\Gamma(^{99m}\text{RhNi})=0.56(5) \text{ MHz} .$$

The ratio of the linewidth to the zero-field splitting is

$$\Gamma/\nu_M(^{99m}\text{RhNi})=2.6(2)\times 10^{-3} .$$

#### D. $^{101m}\text{RhNi}$

Because of the relatively long half-life of  $^{101m}\text{Rh}$  ( $T_{1/2}=4.3$  d) and the convenient hyperfine splitting frequency of  $\sim 200$  MHz the NMR-ON resonances of  $^{101m}\text{RhNi}$  could be measured with very high precision. The NMR-ON resonances for  $B_{\text{ext}}=1, 12,$  and  $20$  kG are shown in Fig. 3. The results are listed in columns 4 and 5 of Table II. For the zero-field splitting and the resonance shift we get, taking the full data set ( $B_{\text{ext}}=1, 3, 6, 12, 15,$  and  $20$  kG)

$$\nu(B_{\text{ext}}=0)=208.618(12) \text{ MHz} ,$$

$$d\nu/dB_{\text{ext}}=-0.9182(10) \text{ MHz/kG} .$$

Taking only the data for  $B_{\text{ext}}=6, 12, 15,$  and  $20$  kG, the results are

$$\nu(B_{\text{ext}}=0)=208.642(14) \text{ MHz} ,$$

$$d\nu/dB_{\text{ext}}=-0.9197(10) \text{ MHz/kG} ,$$

i.e., the resonance shift agrees with the shift of the full data set; the difference is  $2(2)\times 10^{-3}$ . The results for the  $^{101m}\text{RhNi}$  linewidth are

$$\Gamma(B_{\text{ext}}=0)=0.48(3) \text{ MHz} ,$$

$$d\Gamma/dB_{\text{ext}}=0.000(3) \text{ MHz/kG} .$$

Again, the linewidth shows no increase with  $B_{\text{ext}}$ . The average linewidth is

$$\Gamma(^{101m}\text{RhNi})=0.48(2) \text{ MHz} .$$

The ratio of the linewidth to the zero-field splitting is

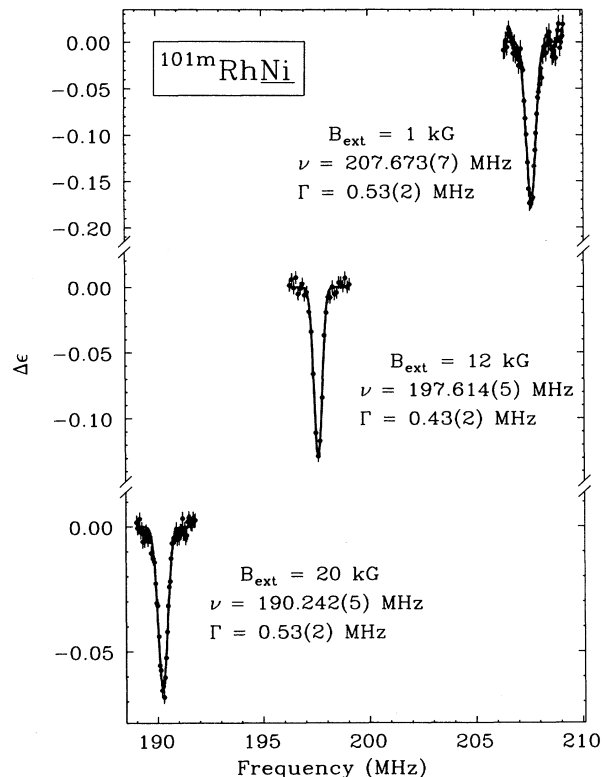


FIG. 3. NMR-ON resonances of the 307 keV transition of  $^{101m}\text{RhNi}$ .

$$\Gamma/\nu_M(^{101m}\text{RhNi})=2.3(1)\times 10^{-3} ,$$

i.e., in good agreement with the respective ratio for  $^{99m}\text{RhNi}$ . The average value for  $^{99m}\text{RhNi}$  and  $^{101m}\text{RhNi}$  is

$$\Gamma/\nu_M(\text{RhNi})=2.4(1)\times 10^{-3} .$$

#### E. $^{52}\text{MnNi}$

NMR-ON resonances of  $^{52}\text{MnNi}$  for  $B_{\text{ext}}=1, 9,$  and  $20$  kG are shown in Fig. 4. The results are listed in columns 6 and 7 of Table II. For the zero-field splitting and the resonance shift we get, taking the full data set ( $B_{\text{ext}}=1, 3, 9, 15,$  and  $20$  kG)

TABLE II. NMR-ON results for  $^{99m}\text{RhNi}$  (341 keV  $\gamma$  line),  $^{101m}\text{RhNi}$  (307 keV  $\gamma$  line), and  $^{52}\text{MnNi}$  (average values for the 744, 935, and 1434 keV  $\gamma$  lines). The systematic error for the magnetic field (see text) is again not included.

$B_{\text{ext}}$ (kG)	$^{99m}\text{RhNi}$		$^{101m}\text{RhNi}$		$^{52}\text{MnNi}$	
	$\nu_c$ (MHz)	$\Gamma$ (MHz)	$\nu_c$ (MHz)	$\Gamma$ (MHz)	$\nu_c$ (MHz)	$\Gamma$ (MHz)
1	215.002(24)	0.60(9)	207.673(7)	0.53(2)	127.147(7)	0.49(2)
3	213.117(24)	0.44(10)	205.869(6)	0.48(2)	126.396(6)	0.52(2)
6	210.309(25)	0.59(9)	203.114(6)	0.46(2)		
9	207.426(33)	0.58(12)			124.057(5)	0.49(2)
12			197.614(5)	0.43(2)		
15	201.716(45)	0.62(16)	194.847(6)	0.44(2)	121.724(5)	0.48(2)
20			190.242(5)	0.53(2)	119.788(5)	0.48(2)

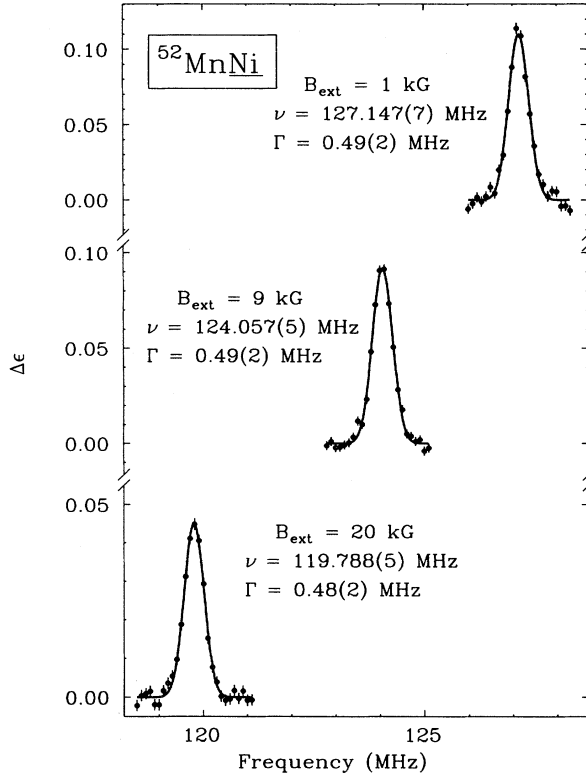


FIG. 4. NMR-ON resonances of  $^{52}\text{MnNi}$  (sum of 744, 935, and 1434 keV transitions).

$$\nu(B_{\text{ext}}=0) = 127.550(5) \text{ MHz} ,$$

$$d\nu/dB_{\text{ext}} = -0.3881(5) \text{ MHz/kG} .$$

Taking only the data for  $B_{\text{ext}} = 3, 9, 15,$  and  $20$  kG, the results are

$$\nu(B_{\text{ext}}=0) = 127.560(5) \text{ MHz} ,$$

$$d\nu/dB_{\text{ext}} = -0.3887(4) \text{ MHz/kG} ,$$

i.e., the resonance shift is in perfect agreement with the shift of the full data set; the difference is  $2(2) \times 10^{-3}$ . Taking only the data for  $B_{\text{ext}} = 9, 15,$  and  $20$  kG, the results are

$$\nu(B_{\text{ext}}=0) = 127.547(11) \text{ MHz} ,$$

$$d\nu/dB_{\text{ext}} = -0.3880(8) \text{ MHz/kG} ,$$

i.e., the resonance shift is in perfect agreement with the shift of the full data set; the difference is  $0(2) \times 10^{-3}$ . The results for the  $^{52}\text{MnNi}$  linewidth are

$$\Gamma(B_{\text{ext}}=0) = 0.50(2) \text{ MHz} ,$$

$$d\Gamma/dB_{\text{ext}} = -0.001(1) \text{ MHz/kG} .$$

Again, the linewidth shows no increase with  $B_{\text{ext}}$ . The average linewidth is

$$\Gamma(^{52}\text{MnNi}) = 0.49(1) \text{ MHz} .$$

The ratio of the linewidth to the zero-field splitting is

$$\Gamma/\nu_M(^{52}\text{MnNi}) = 3.9(1) \times 10^{-3} ,$$

i.e., by a factor of  $1.63(8)$  larger than the respective ratio for  $^{99m,101m}\text{RhNi}$ .

## IV. DISCUSSION

### A. Resonance shifts of Rh and Mn in Fe and Ni

As already mentioned in Sec. II, a (systematic) uncertainty exists for the absolute value of the magnetic field at the sample site. A systematic error of 1% will be included in the *final* values for the resonance shifts and  $K$  values. Throughout the following discussion this error will be omitted as it is the same for all measurements and a better impression of the actual consistency and reproducibility of the resonance shift data is thus obtained.

The results from the shift analysis according to Eq. (4) depend slightly on the field range which is taken into account: Including low-field ( $B_{\text{ext}} < 3$  kG) resonances, the results for the shift are slightly smaller than those obtained from  $B_{\text{ext}} \geq 3$  kG data sets. The difference of the obtained resonance shifts is of the order of several  $10^{-3}$ . We will discuss effects which may cause deviations from the linear connection between  $\nu$  and  $B_{\text{ext}}$  in Sec. IV B. As final results for the resonance shifts we adopt the analyses of the reduced data sets with either  $B_{\text{ext}} \geq 3$  kG or  $B_{\text{ext}} \geq 6$  kG. (If the statistical accuracy is sufficient we take the results from the  $B_{\text{ext}} \geq 6$  kG data sets.) These results are listed in Table III. For  $^{52}\text{Mn}$ , two precise values for the magnetic moment are known,  $\mu = +3.0622(12)\mu_N$  and  $\mu = +3.0632(13)\mu_N$ .<sup>11</sup> Taking the average value, the resonance shift for  $^{52}\text{Mn}$  is expected to be  $0.3891(2) \times (1+K)$  MHz/kG. Thus  $K$  is found to be

$$K_{\text{Fe}}^{(\text{Mn})} = 0(3) \times 10^{-3} ,$$

$$K_{\text{Ni}}^{(\text{Mn})} = -1(1) \times 10^{-3} ,$$

i.e., there is no significant anomaly in the resonance shift of Mn in Fe and Ni. This is in good agreement with the result of other measurements, which are listed in Table IV. In all these experiments the deduced  $|K|$  values have been well below 1%.

For Rh, the hyperfine splitting frequencies and the resonance shift data were analyzed simultaneously via a *least-squares* fit, with the following parameters:  $g(^{99m}\text{Rh}), g(^{100m}\text{Rh}), g(^{101m}\text{Rh}), g(^{102}\text{Rh}), g(^{103}\text{Rh}), g(^{103m}\text{Rh}), g(^{105}\text{Rh}), B_{\text{HF}}(\text{RhFe}), B_{\text{HF}}(\text{RhNi}), K_{\text{Fe}}^{(\text{Rh})}, K_{\text{Ni}}^{(\text{Rh})}$ , and  $^{100m}\Delta_{\text{Fe}}^{103}$  for the hyperfine anomaly between  $^{100m}\text{Rh}$  and  $^{103}\text{Rh}$  (in Fe).

The data set used for the fit is listed in Table V. As results we get for the  $g$  factors and magnetic moments

$$g(^{99m}\text{Rh}) = 1.259(4); \quad \mu(^{99m}\text{Rh}) = 5.668(16) ;$$

$$g(^{101m}\text{Rh}) = 1.216(3); \quad \mu(^{101m}\text{Rh}) = 5.474(16) ;$$

$$g(^{102}\text{Rh}) = 0.673(2); \quad \mu(^{102}\text{Rh}) = 4.041(12) ;$$

$$g(^{103m}\text{Rh}) = 1.297(4); \quad \mu(^{103m}\text{Rh}) = 4.541(14) ;$$

$$g(^{105}\text{Rh}) = 1.272(4); \quad \mu(^{105}\text{Rh}) = 4.452(13) ;$$

TABLE III. NMR-ON results of Rh isotopes. [To demonstrate the high consistency of the data *per se* the systematic error of  $dv/dB_{\text{ext}}$  and  $\nu(B_{\text{ext}}=0)/(dv/dB_{\text{ext}})$ —which is the same for all measurements—is omitted here. For the derivation of final results a 1% systematic error—see text—is assumed.]

System	Sample	$\nu(B_{\text{ext}}=0)$ (MHz)	$dv/dB_{\text{ext}}$ (MHz/kG)	$\nu(B_{\text{ext}}=0)/(dv/dB_{\text{ext}})$ (kG)
$^{101m}\text{RhFe}$	a	516.01(2)	-0.9195(28)	-561.2(1.7)
	b	516.04(3)	-0.9188(47)	-561.6(2.9)
$^{99m}\text{RhNi}$	c	215.98(3)	-0.9502(40)	-227.3(1.0)
$^{101m}\text{RhNi}$	c	208.63(1)	-0.9192(7)	-227.0(2)
	d	208.63(2)	-0.9197(9)	-226.8(2)

<sup>a</sup>This work.

<sup>b</sup>Reference 10.

<sup>c</sup>This work.

<sup>d</sup>Reference 10.

for the hyperfine anomaly

$$^{100m}\Delta_{\text{Fe}}^{103} = 0.037(3) ;$$

for the hyperfine fields

$$B_{\text{HF}}(\text{RhFe}) = -556.5(1.6) \text{ kG} ;$$

$$B_{\text{HF}}(\text{RhNi}) = -225.0(6) \text{ kG} ;$$

and for the  $K$  values

$$K_{\text{Fe}}^{(\text{Rh})} = -0.009(4) ;$$

$$K_{\text{Ni}}^{(\text{Rh})} = -0.009(3) ;$$

$$K_{\text{Fe}}^{(\text{Rh})} - K_{\text{Ni}}^{(\text{Rh})} = 0.001(3) .$$

The negative  $K$  values for Fe and Ni together with the small difference between  $K_{\text{Fe}}^{(\text{Rh})}$  and  $K_{\text{Ni}}^{(\text{Rh})}$  could point to an erroneous hyperfine field which is fixed by the  $g$  factor of  $^{100m}\text{Rh}$  and the hyperfine splitting of  $^{100m}\text{RhFe}$ . Nevertheless,  $|K| \leq 10^{-2}$  is fulfilled. Thus the literature

TABLE IV. Experimental  $K$  values from NMR-ON measurements partly taken from Ref. 10. (The systematic error is again omitted.)

System	$\nu(B_{\text{ext}}=0)$ (MHz)	$dv/dB_{\text{ext}}$ (MHz/kG)	$K \times 10^3$	$B_{\text{ext}}$ (kG)	Ref.
$^{52}\text{MnFe}$	88.77(2)	-0.3892(11)	0(3)	6,11,20	a
	88.76(2)	-0.3878(9)	-3(3)	1,20	b
	88.76(2)	-0.3879(8)	-3(2)	1,11,20	c
$^{52}\text{MnNi}$	127.55(1)	-0.3887(4)	-1(1)	3,9,15,20	a
	127.55(2)	-0.3887(11)	-1(3)	1,11,20	d
$^{54}\text{MnFe}$	190.16(2)	-0.8294(33)	-5(4)	1,6,20	c
$^{56}\text{CoFe}$	210.18(2)	-0.7360(15)	+3(4)	1,6,20	c
$^{58}\text{CoFe}$	441.83(5)	-1.528(12)	-9(8)	1,6,11	c
$^{60}\text{CoFe}$	165.98(1)	-0.5790(6)	0(2)	1,5,10,15,20	e
	166.00(1)	-0.5807(7)	+3(2)	2,6,10	f
$^{60}\text{CoCo}$	125.04(2)	-0.5816(13)	+4(3)	1,6,13,20	g
	125.08(2)	-0.5744(12)	-8(3)	1,6,13,20	h
	125.08(1)	-0.5815(8)	+4(3)	6,9,5,13,16,20	i
	125.18(3)	-0.5821(24)	+5(5)	6,10,16,20	k

<sup>a</sup>This work.

<sup>b</sup>Main experiment:  $^{101m}\text{RhFe}$ .

<sup>c</sup>Main experiment:  $^{89}\text{ZrFe}$ .

<sup>d</sup>Main experiment:  $^{101m}\text{RhNi}$ .

<sup>e</sup>0.1 at. % sample.

<sup>f</sup>0.1 at. % sample; main experiment: MAPON.

<sup>g</sup>Sample indirectly annealed at 900°C.

<sup>h</sup>Sample electrically heated until melting.

<sup>i</sup>Main experiment: MAPON;  $\Gamma = 0.60(2)$  MHz.

<sup>k</sup>Main experiment: MAPON;  $\Gamma = 1.4(1)$  MHz.

TABLE V. Input data for the least-squares fit.

Isotope	Host	$\nu_M$ (MHz)	$d\nu/dB_{\text{ext}}$ (MHz/kG)	$g$	Ref.
$^{99m}\text{Rh}$	Ni	215.984(29)	-0.9502(40)		a
	Fe	534.28(5)			8
$^{100m}\text{Rh}$	Fe	917.1(2.0)		2.162(4)	13
$^{101m}\text{Rh}$	Ni	208.633(9)	-0.9192(7)		a
			-0.9197(9)		10
	Fe	516.008(20)	-0.9195(28)		a
			-0.9188(47)		10
$^{102}\text{Rh}$	Fe	285.66(2)			14
$^{103}\text{Rh}$	Fe	72.35(2)		0.176 80(4)	11,15
$^{103m}\text{Rh}$	Fe	550.3(5)			7
$^{105}\text{Rh}$	Fe	529.62(3)			16
	Ni	218.06(5)			16

<sup>a</sup>This work.

values for  $K$  which grouped around of  $\sim -5\%$  must be erroneous, most probably due to experimental problems which are discussed in Sec. IV B.

Disregarding the literature value for the hyperfine field of  $\text{RhFe}$  as determined via the hyperfine splitting of  $^{100m}\text{RhFe}$  and the  $g$  factor of  $^{100m}\text{Rh}$ , we derive, taking  $K_{\text{Fe}}^{(\text{Rh})} = 0.00(1)$ —all  $K$ -values known experimentally from reliable measurements follow  $|K| \leq 10^{-2}$ —, the following results:

$$g(^{99m}\text{Rh}) = 1.249(13); \quad \mu(^{99m}\text{Rh}) = 5.62(6);$$

$$g(^{101m}\text{Rh}) = 1.206(12); \quad \mu(^{101m}\text{Rh}) = 5.43(6);$$

$$g(^{102}\text{Rh}) = 0.668(7); \quad \mu(^{102}\text{Rh}) = 4.01(4);$$

$$g(^{103m}\text{Rh}) = 1.286(13); \quad \mu(^{103m}\text{Rh}) = 4.50(5);$$

$$g(^{105}\text{Rh}) = 1.261(13); \quad \mu(^{105}\text{Rh}) = 4.41(5);$$

for the hyperfine anomaly

$$^{100m}\Delta_{\text{Fe}}^{103} = 0.046(11);$$

for the hyperfine fields

$$B_{\text{HF}}(\text{RhFe}) = -561(6) \text{ kG};$$

$$B_{\text{HF}}(\text{RhNi}) = -226.9(2.3) \text{ kG};$$

and for the  $K$  values

$$K_{\text{Ni}}^{(\text{Rh})} = 0.00(1);$$

$$K_{\text{Fe}}^{(\text{Rh})} - K_{\text{Ni}}^{(\text{Rh})} = 0.001(3).$$

These are the results which we recommend.

## B. NMR-ON resonance shift

In the NMR-ON technique, radioactive nuclei are oriented at low temperatures, and the hyperfine splitting is detected via the anisotropy of the emitted  $\gamma$  radiation. The NMR-ON “signal” is the change of the  $\gamma$  anisotropy, normally a reduction, in some cases—which are not relevant here—also an increase of the  $\gamma$  anisotropy.

The hyperfine field at the nuclear site has a characteristic distribution (inhomogeneous broadening), which, in

the ideal case, can be described by a Gaussian distribution with width  $\Delta B_{\text{HF}}$ . The NMR-ON signal is a frequency map of this distribution with linewidth  $\Gamma$ , which, according to Eq. (1), is directly correlated with the hyperfine field distribution  $\Delta B_{\text{HF}}$ . (For the moment, the influence of a quadrupole splitting is neglected; this will, however, be discussed below.)

The hyperfine field distribution and hence the linewidth  $\Gamma$  depends on the environment of the probe nuclei. The “minimum” linewidth is obtained if all probe nuclei are located at substitutional lattice sites with an undisturbed surrounding. [“Undisturbed surroundings” means that there are no lattice defects (or only the minimum number of lattice defects according to thermal equilibrium) within a sphere around the probe nuclei with a radius as large as possible.] In this case the hyperfine field distribution can be described by *one* Gaussian line.

It is known, however, that in many experiments linewidths are observed which are (much) larger than the “minimum” linewidth. In this case the linewidth depends on experimental conditions (high impurity concentration, lattice damage by the sample preparation, nonideal annealing). This must be attributed to the fact that the impurity nuclei are (partly) located at (substitutional) lattice sites with one or more lattice defects in the near neighborhood. In this case the structure of the NMR-ON resonance is no more of simple Gaussian type. We will discuss below that, for samples with linewidths larger than the “minimum” linewidth, there are several effects which may simulate a Knight shift. (For completeness it should be added that an additional “experimental” broadening may be introduced by an inhomogeneity of the external magnetic field.)

Let us for the further discussion first assume that we have the best possible sample (without an “experimental” contribution to the line broadening), i.e., that the frequency distribution is a Gaussian with “intrinsic” linewidth  $\Gamma_{\text{in}}$ . There are different contributions to this “minimum” linewidth, which are not understood in detail until now. Only those aspects are discussed below which are relevant in the context of the measurement of resonance shifts with the external magnetic field.

Experimentally, in order to get a resonance signal with reasonable statistical accuracy the applied radio frequency (center frequency  $\nu_{\text{rf}}$ ) must be frequency modulated with a bandwidth  $\Delta_{\text{FM}}$ , which is chosen so that  $\Delta_{\text{FM}}/\Gamma_{\text{in}} = 0.1 \cdots 1$ . In order to get a homogeneous radio-frequency power density over the full modulation bandwidth, a triangular frequency modulation is chosen. Then the power density is  $P_{\text{rf}}/\Delta_{\text{FM}}$ , where  $P_{\text{rf}}$  is the integral rf power. It is obvious that the *observed* linewidth depends on  $\Gamma_{\text{in}}$  and  $\Delta_{\text{FM}}$ . The observed width of the NMR-ON resonance increases with  $\Delta_{\text{FM}}$ . Thus for a precise determination of the resonance center, a small resonance linewidth would be desirable; this would imply a small modulation band width  $\Delta_{\text{FM}}$ . On the other hand, the accuracy with which the resonance center can be determined (via a *least-squares* fit) depends directly on the resonance amplitude, and a large resonance amplitude implies a large  $\Delta_{\text{FM}}$ . Thus  $\Delta_{\text{FM}}$  must always be chosen as a compromise between resonance amplitude and line

broadening.

For the determination of the resonance shift  $d\nu/dB_{\text{ext}}$ , NMR-ON resonance measurements are performed for different values of the external magnetic field  $B_{\text{ext}}$ . For precise measurements,  $B_{\text{ext}}$  should be varied in a range as large as possible. In practice, there are limitations: Magnetic fields up to 20 kG can be obtained easily with a moderately small superconducting (Helmholtz-type) magnet. The experimental NMR-ON resonances are interpreted with a *least-squares* fit. Here the correct theoretical description of the frequency distribution has to be taken into account. Normally, as also in the present case, a Gaussian is taken, with resonance center  $\nu_c$  and linewidth  $\Gamma_{\text{in}}$ , the frequency modulation bandwidth being taken into account by a proper integration. Thus, from the *least-squares* fit, the resonance centers  $\nu_c(B_{\text{ext}})$  and the linewidth  $\Gamma_{\text{in}}(B_{\text{ext}})$  are obtained.

[From measurements with high statistical accuracy it is known experimentally that, for several elements as dilute impurities in Fe and/or Ni—depending on the special features of the metallurgic phase diagram and, possibly, on the sample preparation—the theoretical description with one Gaussian does not describe the NMR-ON spectra completely. There is in many cases an *additional* contribution to the NMR-ON signal resulting from nuclei on lattice sites with a “moderately disturbed” surrounding: This contribution can in many cases be described well by a second Gaussian with a larger intrinsic linewidth. The center of this second distribution is normally shifted towards lower frequencies (with respect to the center frequency of the nuclei on undisturbed lattice sites). In the present case all NMR-ON spectra were interpreted with one and two Gaussians: The obtained center frequency for the sharp line was affected to such a small degree that the final values for the resonance shifts were identical.]

The data set  $\nu_c(B_{\text{ext}})$  is interpreted again with a least-squares fit, now taking the linear dependence of Eq. (3) as theoretical description. [Here it should be added that demagnetization effects have to be considered which depend on the sample geometry. In the case of thin samples the effect can be taken into account by a demagnetization field  $B_{\text{dem}}$  acting antiparallel to  $B_{\text{ext}}$ , which raises from 0 to  $B_{\text{dem}}^{(\text{max})}$  in the magnetization region.  $B_{\text{dem}}^{(\text{max})}$  depends on the ratio of thickness  $x$  to the diameter  $d$  (or a corresponding linear dimension) of the sample. For thin samples (as used in the present work)  $x \sim 1 \mu\text{m}$ ,  $d \sim 4 \text{ mm}$ , i.e.,  $x/d \sim 2.5 \times 10^{-4}$ , the demagnetization field is of the order of  $B_{\text{dem}}^{(\text{max})} \sim 20 \text{ G}$  and can hence be neglected for the shift analyses.] Thus final values for  $\nu_c(B_{\text{ext}}=0)$  and  $d\nu_c/dB_{\text{ext}}$  are obtained. Let us now discuss effects which could have an influence on  $d\nu_c/dB_{\text{ext}}$  and thus yield an incorrect value of  $|g|(1+K)$ .

(i) The *effective* hyperfine field (corresponding to the resonance center  $\nu_c$ ) might depend on  $B_{\text{ext}}$ , at least for the region of  $B_{\text{ext}}$  for which the electronic magnetization is not saturated,  $B_{\text{ext}} < B_{\text{ext}}^{(\text{sat})}$ . It could be expected that the hyperfine field depends (slightly) on the direction of the electronic magnetization with respect to the crystal axes, i.e., the hyperfine fields may be different for the  $\langle 100 \rangle$ ,  $\langle 110 \rangle$ , and  $\langle 111 \rangle$  direction. [Experimental evi-

dence for such an effect might be deduced from NMR-ON measurements on  $^{131}\text{I}$  in Fe single crystals:<sup>12</sup> The substitutional resonance frequencies extrapolated to zero internal field were 683.80(10) MHz for  $B_{\text{ext}} \parallel \langle 100 \rangle$ , 684.04(5) MHz for  $B_{\text{ext}} \parallel \langle 110 \rangle$ , and 683.88(5) MHz for  $B_{\text{ext}} \parallel \langle 111 \rangle$ .] For  $B_{\text{ext}}=0$ , the directions of the magnetic domains point into the direction of easy magnetization, i.e., for Fe, the  $\langle 100 \rangle$  direction. As for the polycrystal sample the  $\langle 100 \rangle$  directions of all domains are distributed homogeneously in space, there is no macroscopic net magnetization for  $B_{\text{ext}}=0$ . The hyperfine field for this case is given by  $B_{\text{HF}} = B_{\text{HF}}^{(100)}$ . In the magnetization regime,  $0 < B_{\text{ext}} < B_{\text{ext}}^{(\text{sat})}$ , the magnetizations of the domains are (finally) rotated into the direction of  $B_{\text{ext}}$ , the electronic magnetization raises until its saturation value is obtained for  $B_{\text{ext}} = B_{\text{ext}}^{(\text{sat})}$ . In this region, the hyperfine field is given by

$$B_{\text{HF}} = a^{(100)} B_{\text{HF}}^{(100)} + a^{(110)} B_{\text{HF}}^{(110)} + a^{(111)} B_{\text{HF}}^{(111)},$$

where  $a^{(100)}$ ,  $a^{(110)}$ , and  $a^{(111)}$  are coefficients which depend on the *average* angles between the electronic magnetization and the  $\langle 100 \rangle$ ,  $\langle 110 \rangle$ ,  $\langle 111 \rangle$  directions, respectively. Thus the effective magnetic hyperfine field might change (slightly) in the magnetization region. (This would be accompanied by a field-dependent linewidth in the magnetization region; see discussion below.) For  $B_{\text{ext}} > B_{\text{ext}}^{(\text{sat})}$ , however,  $a^{(100)}$ ,  $a^{(110)}$ , and  $a^{(111)}$  remain constant, which means, that  $B_{\text{HF}}$  remains constant, too. Thus, from this effect, no artificial contribution to the resonance shift is introduced for  $B_{\text{ext}} \geq B_{\text{ext}}^{(\text{sat})}$ .

(ii) In the magnetization region, the lattice constants may change (slightly) due to magnetostriction. Thus the *s*-electron spin density at the nuclear site and hence the hyperfine field may change as function of  $B_{\text{ext}}$ . This could cause a spurious contribution to the resonance shift for  $0 < B_{\text{ext}} < B_{\text{ext}}^{(\text{sat})}$ . For  $B_{\text{ext}} > B_{\text{ext}}^{(\text{sat})}$ , magnetostriction should no more change, and the resonance shift should not be influenced.

(iii) In the magnetization regime, a “trivial” effect actually *must* influence the shift: In this regime, the electronic magnetization of the domains is not aligned in the direction of  $B_{\text{ext}}$ . This means that the effective magnetic field at the nuclear site is given by a vector addition of  $B_{\text{ext}}$  and  $B_{\text{HF}}$ . Assuming that the average angle between  $B_{\text{ext}}$  and  $B_{\text{HF}}$  is  $\theta_a$ —there exists, of course, a certain distribution for  $\theta_a$ —the effective external magnetic field is (to first order) given by  $B_{\text{ext}} \cos \theta_a$ , where  $\cos \theta_a$  increases with  $B_{\text{ext}}$  until it reaches 1 for  $B_{\text{ext}} \geq B_{\text{ext}}^{(\text{sat})}$ . The influence on the resonance center is complicated as a nonlinear mapping partly compensates the effect: With increasing  $\theta_a$ , the  $\gamma$  anisotropy of the respective nuclei decreases, and the (perpendicular) component of the rf field which induces the rf transitions decreases with  $\cos \theta_a$ , i.e., the NMR-ON detection efficiency decreases with increasing  $\theta_a$ . It is, however, easy to avoid the spurious shift due to this effect by taking only  $B_{\text{ext}} > B_{\text{ext}}^{(\text{sat})}$  NMR-ON resonances for the resonance shift analysis. In this context, it is sometime speculated<sup>17</sup> that the “true”  $B_{\text{ext}}^{(\text{sat})}$  is far above the field for which the  $\gamma$  anisotropy is saturated (typically 0.5–2 kG, depending on the specific properties



of the sample). Our experimental results do not support this speculation; we discuss this problem in the context of large experimental linewidths below.

(iv) It has been observed for several impurity-host systems that the linewidth increases with the external magnetic field. (We will exclude here that this increase is caused by the inhomogeneity of the external magnetic field. This will be discussed later.) Let us first discuss the expected linewidth in the magnetization region,  $0 < B_{\text{ext}} < B_{\text{ext}}^{(\text{sat})}$ . There are two different "trivial" effects: (a) Because of the distribution of the effective external magnetic fields  $B_{\text{ext}} \cos\theta$  at the nuclear sites according to the spread of  $\theta$  around the average  $\theta_a$ , a larger linewidth would be expected with respect to the linewidth for  $B_{\text{ext}} > B_{\text{ext}}^{(\text{sat})}$ . (b) If the hyperfine fields are different for the  $\langle 100 \rangle$ ,  $\langle 110 \rangle$ ,  $\langle 111 \rangle$  directions, respectively, as discussed before, an increase of the linewidth with  $B_{\text{ext}}$  would be expected until the maximum broadening is obtained for  $B_{\text{ext}} = B_{\text{ext}}^{(\text{sat})}$ . If the experimentally observed increase of the linewidth were due to this effect, the NMR-ON resonance shift in the magnetization region would be expected to deviate considerably from the shift obtained for  $B_{\text{ext}} > B_{\text{ext}}^{(\text{sat})}$ . This deviation would be expected to be of the order of  $\Delta\Gamma$  (the difference of high-field and low-field linewidths), which contradicts the experimental observation that the deviations of the resonance centers in the magnetization region (with respect to the extrapolation from high-field resonances) are much smaller than the changes of the resonance widths. These effects are, however, again not relevant if only  $B_{\text{ext}} > B_{\text{ext}}^{(\text{sat})}$  NMR-ON resonances are taken for the resonance shift analysis.

There is, however, also a "nontrivial" effect, which may cause an external-magnetic-field dependence of the observed linewidth. Even for the "best" samples, there are differences in the magnetic environments of the probe nuclei, and, the different magnetic environments may cause different *local* inhomogeneous linewidths. As the enhancement factor for the rf field also depends on the magnetic environment, a different weighting of the different contributions to the resonance signal may occur due to the magnetic-field dependence of the rf-enhancement factor. If the average hyperfine splitting depends on the specific properties of the magnetic environment, a magnetic-field-dependent resonance offset is introduced, even for  $B_{\text{ext}} > B_{\text{ext}}^{(\text{sat})}$ . To detect this effect, NMR-ON measurements must be performed varying the rf power for fixed external magnetic field.

(v) In principle, the mapping of the hyperfine field distribution to the measured NMR-ON frequency distribution might contain a nonlinear component. This could be caused by the variation of the spin-lattice relaxation time within the resonance region, and since the spin-lattice relaxation time is known to be dependent on the external magnetic field, the nonlinearity of the hyperfine field-frequency mapping could be dependent on  $B_{\text{ext}}$ . In this way shifts of the resonance centers dependent on  $B_{\text{ext}}$  could be caused. We have therefore measured the frequency dependence of the spin-lattice relaxation time over the full resonance region for several (highly dilute)  $^{60}\text{CoFe}$  samples with high precision<sup>18</sup>. No frequency dependence of the spin-lattice time was detected. Thus

we must conclude that the influence on the resonance shift due to *this* effect is negligibly small.

(vi) There are several possibilities for the occurrence of an electric-field gradient (EFG) in *cubic* Fe and Ni: (a) (Weak) symmetry breaking of the cubic symmetry via magnetostriction. The resulting EFG is collinear with the magnetization and hence collinear with the magnetic hyperfine interaction. (b) An unquenched orbital momentum of the *nd* electrons at the site of the probe nuclei due to the spin-orbit interaction. Here again, the resulting EFG is collinear with the magnetic hyperfine interaction. Only in few cases, e.g., for the 5d elements Au and Ir in Fe and Ni, this EFG is so large that the resonance substructure could be resolved in several favorable cases of low-spin states. In most cases, however, the quadrupole substructure cannot be resolved. In these cases, an additional broadening of the NMR-ON resonance may be introduced by the unresolved quadrupole interaction, even for samples with the "best" magnetic properties.

In the presence of such an additional electric quadrupole interaction, the magnetic resonance as described by Eq. (2) is split into a set of  $2I$  subresonances, which are separated by

$$\Delta\nu_Q = 3\nu_Q / [2I(2I-1)]. \quad (8)$$

Here  $\nu_Q$  is the quadrupole interaction frequency defined as

$$\nu_Q = e^2qQ/h, \quad (9)$$

where  $Q$  is the nuclear spectroscopic quadrupole moment and  $eq$  is the electric-field gradient acting at the nuclear sites. If the subresonance separation is smaller than the (magnetic) linewidth, the effective resonance center is shifted with respect to the case without electric quadrupole interaction by

$$\overline{\Delta\nu} = \sum_{m=-I}^{I-1} A_m^{m+1} (m+1/2) \Delta\nu_Q. \quad (10)$$

Here  $A_m^{m+1}$  is the subresonance amplitude for the transitions between state  $|m\rangle$  and  $|m+1\rangle$ , which depends on the temperature  $T$ , the rf power  $P_{\text{rf}}$  and the frequency modulation bandwidth  $\Delta_{\text{FM}}$  [The dependence on  $\Delta_{\text{FM}}$  is twofold: (a) Only those subresonances can be affected which lay within the frequency modulation bandwidth; (b) The relative amplitudes  $A_m^{m+1}$  depend on the rf power density  $P_{\text{rf}}/\Delta_{\text{FM}}$ .]

It is a matter of fact that saturation of the resonance (for high external magnetic fields) is normally achieved only for selected systems (with long spin-lattice relaxation times). Thus, essentially due to the magnetic-field dependence of the enhancement factor for the rf field and the magnetic-field dependence of the spin-lattice relaxation time, the presence of an electric quadrupole interaction causes external-magnetic-field-dependent resonance offsets and hence a spurious resonance shift. (From detailed measurements on the quadrupole-interaction-resolved NMR-ON spectrum of  $^{192}\text{IrNi}$  it was demonstrated that the relative subresonance amplitudes actually depend on the external magnetic field,<sup>6</sup> i.e., that an influence on the resonance shift of the resonance centers

of unresolved resonances *must* occur.]

The resonance offsets are of the order of  $\Delta\nu_Q$ ; thus a systematic error of  $K$  of the order of  $\Delta\nu_Q/\Delta\nu^{\text{mag}}$  *must* be expected, where  $\Delta\nu^{\text{mag}}$  is the total resonance shift by the magnetic field. This has been the reason for the misinterpretation of the resonance shifts of  $^{191\text{m}}\text{Ir}$  and  $^{192}\text{Ir}$  in Fe and Ni and  $^{198}\text{Au}$  in Fe,<sup>3</sup> which are systems with large quadrupole splittings and short spin-lattice relaxation times.

In those cases, the NMR-ON resonances which are taken for a resonance-shift analysis have to be measured under the same experimental conditions, which means that (at least) the rf power has to be adjusted for each value of the magnetic field so that the magnetic-field dependence of the rf-enhancement factor and of the spin-lattice relaxation are compensated. [For  $^{191\text{m}}\text{IrNi}$  (Ref. 3) the deviation of the resonance shift is essentially due to the unresolved quadrupole interaction, incomplete reorientation in the intermediate state, together with the magnetic-field dependence of the spin-lattice relaxation time and the enhancement factor. In such cases a quadrupole-splitting-induced contribution to the resonance shift *must* occur, which *cannot be compensated* by variation of experimental parameters. In such cases, the large  $K$  values ( $\sim 0.15$  for  $^{191\text{m}}\text{IrNi}$ , Ref. 3) are exactly reproducible.]

(For Rh in Fe and Ni, no dependence of the resonance centers on the modulation bandwidth and the temperature was observed. In addition, the quadrupole splitting of  $^{101\text{m}}\text{RhFe}$  was measured with the modulated adiabatic passage on oriented nuclei (MAPON) technique.<sup>19</sup> The result was  $\Delta\nu_Q/\Delta\nu^{\text{mag}} \sim 2 \times 10^{-3}$ , i.e., so small that, on the level of  $10^{-2}$ , no appreciable influence on the resonance shifts is to be expected. The details of these measurements, which are not relevant for the present work, will be published elsewhere).

Let us now discuss the case that the experimental linewidth is (much) larger than the "minimum" linewidth. To our knowledge, only the data from such experiments are responsible for the large scattering of resonance shift data in the literature. Systematic NMR-ON studies of  $\text{CoFe}$  samples,<sup>18</sup> which contained different Co concentrations  $c$  in the range between 0.01 and 25 at. %, but which were prepared in the same way, showed a strong dependence of the NMR-ON linewidth as a function of the Co concentration. With increasing impurity concentration, the linewidths increased. In addition, the zero-field splitting frequency was found to be concentration dependent, too. The resonance shifts of the samples with  $c \leq 0.3$  at. % were consistent with  $|K| = 0(1) \times 10^{-2}$ . The samples with higher Co concentrations showed larger linewidths and resonance shifts which were considerably larger than the resonance shifts of the samples with small Co concentration (and small NMR-ON linewidths). E.g., for the 1 at. % sample, a satellite resonance can be resolved which is  $\sim 2$  MHz above the main resonance, with a relative intensity of 14(2)%. The resonance shift of the satellite resonance was  $\sim 10\%$  higher than the resonance shift of the main resonance. (Both resonances, which were well resolved, were measured simultaneously as function of the external magnetic

field.) For higher Co concentration, the resonance shift increased monotonically with the Co concentration.

Thus, the hyperfine field of the individual probe nuclei depends on the neighbors in the lattice. A difference in the neighborhood may cause a decrease or an increase of the effective hyperfine field, depending on the type of the neighbor. Thus, a large NMR-ON linewidth points to *different* neighborhoods of the individual probe nuclei. It is the *difference of the neighborhood*, which may cause an *additional* resonance shift.

(i) The *local* magnetization properties depend on the environment. Thus the enhancement factor for the rf field is different over the entire resonance region. This has the consequence that, as the enhancement factor changes with the magnetic field, the *resonance structure* may change with  $B_{\text{ext}}$ . In general, the functional dependence of the resonance structure on frequency is not known in detail. In the case of the undisturbed substitutional lattice site this can be described by one or more additional Gaussian lines. Such a description may no longer be a good approximation for samples in which the magnetic environments of the probe nuclei are distributed quasicontinuously. Then the change of the resonance structure with  $B_{\text{ext}}$  is unobservable. A change of the resonance structure may, however, cause a hidden (additional) shift of the (effective) resonance centers in the approximation with a discrete set of Gaussians.

(ii) Because of the different magnetic environments of samples with a large experimental linewidth, the spin-lattice relaxation time may now actually vary over the resonance region. Thus, the differential resonance amplitudes within the resonance structure may change with the external magnetic field, by which a magnetic-field dependence of the effective resonance center is immediately introduced.

(iii) Because of symmetry breaking of the cubic symmetry at the probe site by distortions of the lattice (in the near neighborhood) a lattice EFG is produced. For the 3d and 4d elements in Fe and Ni, this lattice EFG may be considerably larger than the EFG due to the unquenched orbital momentum. Thus, a (considerably large) electric quadrupole splitting may be present. The principal axes system of this quadrupole splitting is correlated with the location of the generating lattice distortion. Thus, the angles between the principal  $c$  axis of the EFG and the magnetic hyperfine field may be distributed statistically. In first approximation, this yields an (asymmetric) broadening of the resonance structure and *no* resonance offset of the effective resonance center. It is the difference in the environments and the dependence of the relative amplitudes of the (unresolved) quadrupole subresonances on the enhancement factor for the rf field, that a magnetic-field dependence of the effective resonance center is introduced, causing a spurious contribution to the resonance shift. The quadrupole interaction can, however, be determined with the MAPON method, even if it is much smaller than the inhomogeneous linewidth. Actually, even the distribution of EFG's is accessible with this method. Here it should be added that a magnetic-field dependence of the (effective) electric quadrupole interaction has been observed in several cases.

This yields an additional magnetic-field-dependent contribution to the resonance offset and hence a spurious component to the resonance shift.

Thus, in all cases for which the observed linewidth is larger than the "minimum" linewidth, the origin for this must be ascribed to a lattice distortion (damage) in the vicinity of the probe nuclei. [In the case of an additional (unresolved) quadrupole interaction due to a local-moment-induced electric-field gradient the minimum linewidth depends on the temperature because of temperature dependence of the relative subresonance amplitudes.] Then, a lattice EFG must be expected, leading to resonance offsets and a spurious contribution to the resonance shift, if the effect is not taken into account properly. [In principle, these resonance offsets can be determined by NMR-ON measurements with different temperature, rf power, and modulation bandwidth, and/or additional MAPON measurements. This has not been done in those cases for which  $|K| \geq 0(1) \times 10^{-2}$  had been found.]

## V. CONCLUSIONS

There has been a controversial discussion of NMR-ON resonance shifts in the literature and it has been argued that the "true" resonance shift can be determined (only) from measurements in high magnetic fields.<sup>4,5</sup> In our opinion, these conclusions were drawn from measurements on samples, for which the lower limit of the linewidth, which we denote as "minimum" linewidth, was not reached. Then, however, many effects exist which influence the resonance centers, i.e., which may cause external-magnetic-field-dependent resonance offsets. Collecting the data of  $\sim 20$  resonance shift measurements, partly on the same systems, we found that *all* data were consistent with  $|K| \leq 10^{-2}$ . Thus we conclude that all (actual) Knight shifts are smaller than  $\sim 10^{-2}$ .

For more stringent conclusions the NMR-ON measurements on "minimum-linewidth samples" would have to be performed up to larger external magnetic fields.

Finally we would like to mention that, depending on the specific impurity-host combination, even the "minimum" linewidth of nuclei on substitutional sites with an undisturbed surrounding may be dependent on the external magnetic field. In a recent NMR-ON investigation of Tc isotopes in Fe, such a magnetic-field dependence on the linewidth has been observed, both for <sup>95</sup>TcFe and <sup>96</sup>TcFe. For <sup>52</sup>Mn in the same sample no magnetic-field dependence of the linewidth was found.<sup>20</sup>

It should be added that the inhomogeneous linewidths of impurity systems are not understood in detail until now. Here the electronic properties of the impurity seem to be important. From the observation of small linewidths for noble gases as impurities in Fe it has been speculated that the linewidths arise (partly from) valence fluctuations.<sup>21</sup> On the other hand, it is more likely that spin waves indirectly influence local-spin fluctuations and hence fluctuations of the hyperfine field. It cannot be anticipated *a priori* that such fluctuations induce a symmetric broadening. On the other hand, the observation of  $|K| \leq 10^{-2}$  is an indication that the effect is actually small. Summarizing, we state that, in our opinion, NMR-ON resonance shifts can well be measured reliably with a precision of  $\lesssim 10^{-2}$ . Within this precision no anomaly in the resonance shift is established.

## ACKNOWLEDGMENTS

We wish to thank E. Smolic for experimental help. This work was funded by the German Federal Minister for Research and Technology (BMFT) under Contract No. 06 TM 353/TP 4, by the Deutsche Forschungsgemeinschaft (DFG) under Contract No. Ha 1282/3-1, and, partly, by the Kernforschungszentrum, Karlsruhe.

<sup>1</sup>E. Matthias and R. J. Holliday, Phys. Rev. Lett. **17**, 897 (1966).

<sup>2</sup>R. Laurenz, E. Klein, and W. D. Brewer, Z. Phys. **270**, 233 (1974).

<sup>3</sup>E. Hagn and G. Eska, *Proceedings of the International Conference on Hyperfine Interactions Studied in Nuclear Reactions and Decay, Uppsala, 1974*, edited by E. Karlsson and R. Wäppling (Upplands Grafiska AB, Uppsala, 1974), p. 148 ff.

<sup>4</sup>N. Yazidjoglou, W. D. Hutchison, and D. H. Chaplin, Hyperfine Interact. **75**, 283 (1992).

<sup>5</sup>N. Yazidjoglou, W. D. Hutchison, and D. H. Chaplin, J. Phys. G **5**, 129 (1993).

<sup>6</sup>E. Hagn, K. Leuthold, E. Zech, and H. Ernst, Z. Phys. A **295**, 385 (1980).

<sup>7</sup>H. Kempter and E. Klein, Z. Phys. A **281**, 341 (1977).

<sup>8</sup>R. Eder, E. Hagn, and E. Zech, Phys. Rev. C **32**, 1707 (1985).

<sup>9</sup>K. Nishimura, S. Ohya, and M. Matsuuro, Nucl. Phys. A **451**, 233 (1986).

<sup>10</sup>B. Hinfurtner, C. König, G. Seewald, and J. Herker (unpublished).

<sup>11</sup>P. Raghavan, At. Data Nucl. Data Tables **42**, 189 (1989).

<sup>12</sup>D. Visser, L. Niesen, H. Postma, and H. de Waard, Phys. Rev. Lett. **41**, 882 (1978).

<sup>13</sup>E. Matthias, D. A. Shirley, N. Edelstein, H. J. Körner, and B. A. Olsen, in *Hyperfine Structure and Nuclear Radiations*, edited by E. Matthias and D. A. Shirley (North-Holland, Amsterdam, 1968), p. 878.

<sup>14</sup>B. Hinfurtner, E. Hagn, and E. Zech, Nucl. Phys. A **504**, 467 (1989).

<sup>15</sup>M. Kontani, M. Ota, and Y. Masuda, J. Phys. Soc. Jpn. **29**, 1194 (1970).

<sup>16</sup>E. Hagn, J. Wese, and G. Eska, Phys. Rev. C **23**, 2683 (1981).

<sup>17</sup>D. Chaplin (private communication).

<sup>18</sup>R. Beck, Ph.D. thesis, TU München, 1987.

<sup>19</sup>P. T. Callaghan, P. J. Back, and D. H. Chaplin, Phys. Rev. B **37**, 4900 (1988).

<sup>20</sup>B. Hinfurtner, E. Hagn, E. Zech, W. Tröger, and T. Butz, Z. Phys. A **350**, 311 (1995).

<sup>21</sup>R. Eder, E. Hagn, and E. Zech, Z. Phys. A **326**, 255 (1987).